Preparation and Radar Wave Absorbing Characterization of Bicomponent Fibers with Infrared Camouflage

Bin Yu,[1] Lu Qi,[1] Jian-zhong Ye,[1] Hui Sun[2]

[1]*Research Institute of Biological and Spinning Materials, Tianjin Polytechnic University, Tianjin 300160, China*
[2]*School of Materials Science and Engineering, Tianjin University, Tianjin 300072, China*

Received 18 September 2005; accepted 20 May 2006
DOI 10.1002/app.24854
Published online in Wiley InterScience (www.interscience.wiley.com).

ABSTRACT: Sheath-core bicomponent fibers were prepared by a general melt-spinning method with polypropylene chips and various particles. The melt-spun fibers were characterized by DSC and mass specific electrical resistance (MSER) apparatus. The electromagnetic constant was measured using a network analyzer and the absorbing wave effect was evaluated by an arch method. The results of the DSC thermogram indicated that the crystallinity of polypropylene containing particles in the core-part slightly increased first and then kept steadily with the particles content increase. Nanoparticles in the sheath-part did not make the crystallinity of fibers change markedly. The MSER of fibers rapidly decreased with the metal particles input. The complex permeability of fibers with Ba/Mn-Zn ferrite was improved compared with that of fiber with single Mn-Zn ferrite and the complex permittivity of fiber containing the 20 wt % Ba/Mn-Zn ferrite increased with the increasing bronze content. The fibers filled with the Ba/Mn-Zn ferrite and bronze particles had good radar absorbing effect. The input of Al particles in the sheath-part of the fibers showed a limited effect on the radar wave absorbing properties of the fibers. The lowest infrared emissivity of the fibers including 15 wt % Al particles in sheath-part reached 0.62. © 2007 Wiley Periodicals, Inc. J Appl Polym Sci 104: 2180–2186, 2007

Key words: organic–inorganic composite; polypropylene; bicomponent fibers; radar-absorbing properties; infrared camouflage

INTRODUCTION

The radar signal strength, scattered from a target, determines its detectability. This pertains to the radar cross section (RCS), which frequently should be reduced. Radar-absorbing material (RAM) is a very effective means of RCS reduction in the context of camouflage technology. The basic design theories of RAM, such as Salisbury screen theory, Jaumann absorber theory, etc. were published from early 1950s onwards. But these theoretical studies abated, recently, the main research topic being transferring toward the development of loss material.[1,2] There are electro loss and magnetic loss materials having different advantages and disadvantages, each of which can be used as a mixture[3]; however, the magnetic loss material and coating materials[4] are usually base one, heavy weight of the material is still a concerning problem. To remedy this problem, more and more researches about RAM have been concentrated on fiber materials.[5,6] A number of researches have been carried out, which include spinning of electrically conducting fibers,[7] coating fibers with electrically conducting materials such as metals[8] or conducting polymers and textiles coated with conducting polymers.[9,10]

Correspondence to: L. Qi (qilu7712@163.com).

Journal of Applied Polymer Science, Vol. 104, 2180–2186 (2007)

Recently, there have been great interests in the design of RAM with infrared camouflage.[11,12] However, to the best of our knowledge, there are no reported experimental results on the design of fibers RAM with infrared camouflage. In this article, we designed a radar-absorbing fibers with infrared camouflage effect. For the purpose, we have prepared a bicomponent fiber with sheath-core structure using polypropylene (PP) chips and various fillers.

EXPERIMENTAL

Materials

Barium (Ba) hexaferrite, manganese-zinc(Mn-Zn) cubic ferrite provided from Beijing Central Iron and Steel Research Institute (Beijing, China) and rich bronze powder supplied by Wuxi Gold Powder Factory (Wuxi, China) were used as radar-absorbing agents in the core-part. The mean diameter of all the radar-absorbing agents was ~ 3 μm. The aluminum nanoparticles with 50 nm particle size provided by Wuxi Weifu Group (Wuxi, China) were filled into the sheath-part for infrared camouflage. Each type of specimen is denoted by the particle contents by weight and volume percentage in core-part and sheath-part of the fibers as shown in Table I. Polypropylene chips (isotactic PP) was provided from Shanghai Petro Chemical, China. Its characteristics commonly used for fibers spinning are as follows; M_n: 1.7×10^5, MI: 39.0 g/10 min,

TABLE I
Specimen Denotations of Bicomponent Fibers

	C0S0	C20S0	C40S0	C20S5	C20S10
Contents of particle in the core part of the fibers (wt %/vol %)	0	20/5.01	40/12.38	20/5.01	20/5.01
Contents of particle in the sheath part of the fibers (wt %/vol %)	0	0	0	5/2.22	10/5.56

C means the core part; S means the sheath part.

density: 0.92 g/cm^3, and polydispersity: 3.8. For easier spinning process, PP/fillers master-batches were prepared by a conventional twin-screw extruder.

Spinning process and machine

The spinning machine was a general conjugate spinning machine that was composed of two extruders ($L/D = 25$, $D = 20$ mm) and gear pumps. Both core-part radar master-batches and sheath-part infrared master-batches were dried for at least 2 h at 100°C in vacuum drier to secure complete moisture-free state. The infrared camouflage master-batches were added in the sheath-section and the radar camouflage master-batches were added in the core-section. The fibers sheath-core ratio were 40/60 (w/w) controlled through adjustment of the speed of gear pumps. Two kinds of master-batches were melted in both cylinders, combined in the spinneret. Then, they were extruded through the mononozzles, which have diameter of 0.4 mm.

The Figure 1 illustrates the spinning system used for generating sheath-core bicomponent fibers. The processing temperatures are listed in Table II.

Thermal analysis

For thermodynamic experiment, dynamic scanning calorimerer (DSC, Perkin–Elmer DSC-7) equipped with a cooler was used under the nitrogen atmosphere. All the samples were heated from 0 to 250°C at 10°C/min. From this procedure, the melting temperature (T_m) of the fibers was obtained and apparent enthalpies of fusion were calculated from the area of the endothermic peak. The percent crystallinity of polypropylene was evaluated using the following equation:

$$\text{Crystallinity } (\%) = \frac{\Delta H_f}{\Delta H_f^0 \omega_f}$$

where ΔH_f is the heat of fusion of PP fibers, ω_f is the weight fraction of PP in the blends, and ΔH_f^0 is the extrapolated value of the enthalpy corresponding to the heat of fusion of 100% crystalline PP taken as 209 kJ/kg from the literature.[13]

Electro characterization of the fiber

The electrical resistance of the bicomponent fibers test were performed using fiber mass specific electrical resistance apparatus (MSERA, YG321) at 25°C, 65 HR%.

Electromagnetic parameters of the fibers

The fiber was made into needle-punched nonwoven which was cut into a toroid of outer diameter 7 mm and inner diameter 3 mm. The material permittivity and permeability (ε', ε'', μ', μ'') of the toroidal sample were measured using a network analyzer (HP 8722ES).

Performance test of radar-absorbing

The performance test of radar-absorbing was evaluated by reflectivity using Arch method. Reflectivity R is the ratio of radar-absorbing material (RAM) reflective power to metallic plate reflective power, which can be expressed as:

$$R = \frac{P_a}{P_m}$$

where P_a is the reflective power of the sample and P_m is the reflective power of metallic plate.

In practice, we surveyed the ratio of the reflective power of the sample and the reflective power of metallic plate to the same reference signal that was in direct proportion to transmit, respectively.

$$R_m = \frac{P_m}{P_i}, R_a = \frac{P_a}{P_i}$$

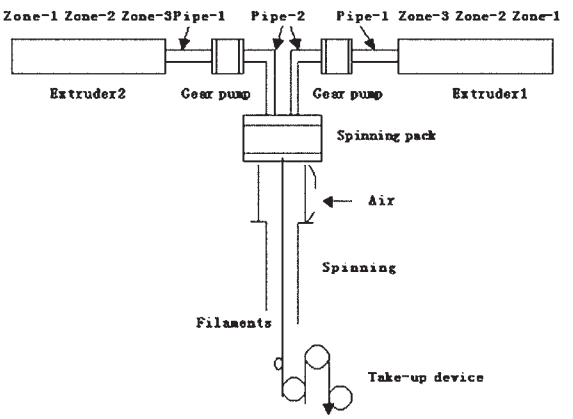

Figure 1 Schematic diagram for the bicomponent fiber spinning system.

TABLE II
Processing Temperature (°C) for Generating Sheath–Core Bicomponent Fibers[a]

	Pack	Pipe-2	Gear pump	Pipe-1	Clamp	Zone-3	Zone-2	Zone-1
Temperature (°C)	255	250	240	240	240	240	240	150

[a] Refer to Figure 1 for illustration.

where P_i is the reference signal. So

$$R = \frac{P_a}{P_m} = \frac{P_a/P_i}{P_m/P_i} = \frac{R_a}{R_m}$$

The Reflectivity was finally expressed with dB as:

$$R_{\mathrm{dB}} = 10\ 1^{\circ}\mathrm{g}R_a - 10\ 1^{\circ}\mathrm{g}R_m$$

The schematic diagram of the experimental setup is shown in Figure 2. The reflectivity of the samples were measured and compared with that from a plane metallic plate. Measurement was carried out using an HP 8757E network analyzer in the swept frequency range from 2 to 18 GHz. Unwound fibers and nonwoven with 380 g/m^2 surface density were made into 180 mm × 180 mm to cover the metallic plate.

Performance test of infrared emissivity of the fibers

The infrared camouflage properties were evaluated by infrared emissivity. The infrared emissivity was measured with 5DX Fourier infrared spectroscopic instrument, infrared emissivity appurtenances for computing the infrared emissivity (NICOLEK, America) and black-body oven (JD-1) at 100°C, wavelengths from 5 to 25 μm. The infrared emissivity is expressed as: $\varepsilon = \varepsilon_1/\varepsilon_2$, where ε_2 is the radiant intensity of fiber and ε_2 is radiant intensity of the black-body oven.

RESULTS AND DISCUSSION

Thermal property

Differential scanning calorimetry thermograms of all the fibers are depicted in Figure 3. Figure 3(a) shows three curves of the DSC thermogram profile of fibers containing ferrite and bronze in the core-part. Figure 3(b) shows two curves of fibers containing nanometer Al particles in the sheath-part. Table III summarizes the data from DSC. In DSC graphs, the melting point (T_m) and crystallinity of fibers including ferrite and bronze in the core-part increased slightly at first and then did not change remarkably with increasing powder content. This can be explained as follows. Low content ferrite and bronze particles acted as nucleating agents and internal plasticizer which made for the regular arrange of macromolecular which resulted in the increase of crystallinity of fibers. However, with the increasing ferrite and bronze content, abundant particles acted as the impurities baffle the movement of the macromolecules and affect the growth of crystal, which lead the crystallinity not to increase. The weight percent crystallinity of PP was calculated via the standard heat of crystallization that was taken to be 209 J/g. Recently, Sang and Sung[14] reported that the addition of the nanometer silver made the crystallinity of fibers to reduce. However, in case of our results, the behavior of PP crystallization in the matrix led to a different result. The crystallinity of fiber with the Al particles did not vary significantly, which revealed[15,16] that nanoparticles Al had two effects on the crystallization of PP: (1) the Al acted as a nucleation site, accelerating the process of PP crystallization; (2) the interaction between PP and the Al impeded the free motion of the PP molecular chains.

The electrical resistivity of the fibers

The mass specific electrical resistivity (MSER) of fibers filled with bronze particles was shown in Figure 4. It was obvious that the MSER of fibers reduced at the low bronze content, but it began to increase after the metal content reached 20%. This can be explained by the nonhomogeneous morphological structure of the fibers with various content fillers. Two phases exist: bronze particles and PP regions. As Faez et al.[17] previously reported, a degree of connectivity between the conductive additives must exist to facilitate the electro conduction. The connectivity between the bronze particles began to form among the PP with the addition of bronze particles. So the MSER reduced rapidly. But too many bronze particles made the compatibility of bronze with PP become bad and some bronze particles formed into conglomerations resulting in the connec-

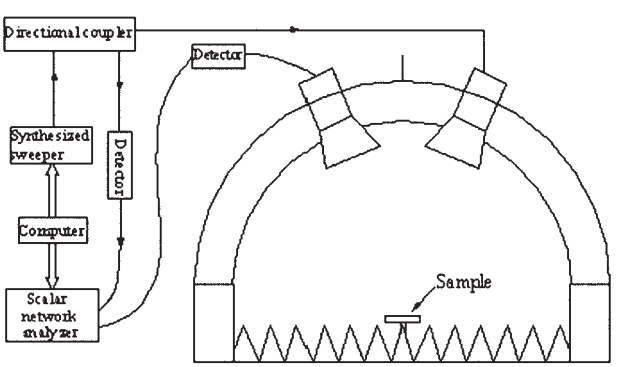

Figure 2 Reflectivity measurement setup of arch method.

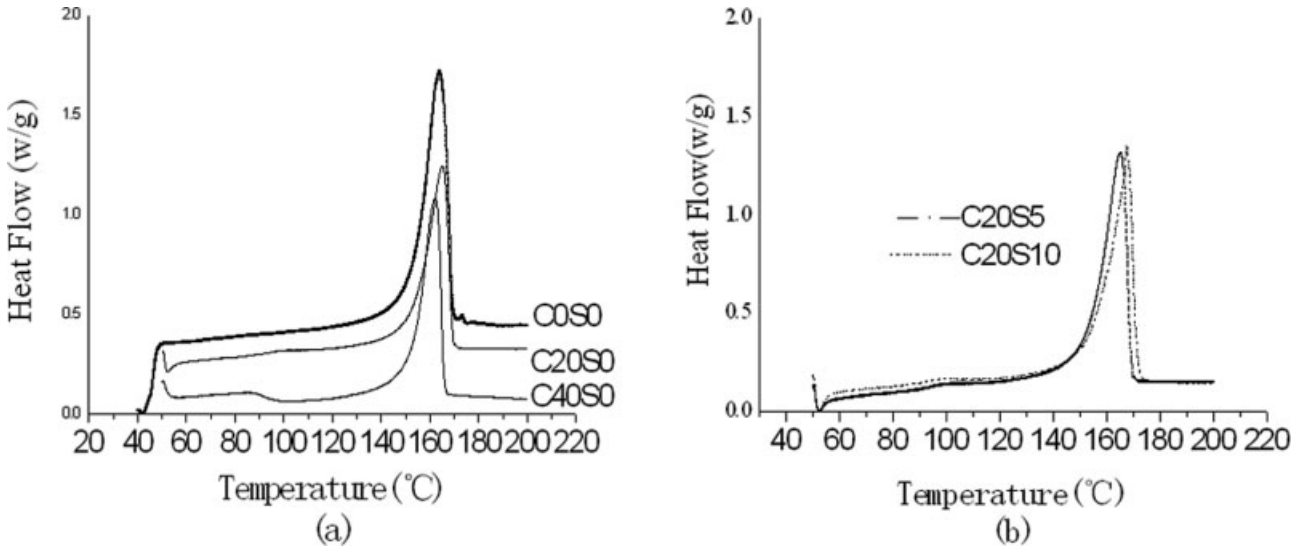

Figure 3 DSC of spun fibers of varying fillers concentration; (a) fibers containing common particles in the core-part, (b) fibers containing nanometer particles in the sheath-part.

tion between bronze particles breaking and MSER increase.

The radar wave absorption properties and electromagnetic parameters of the fibers

The Figure 5 indicates that the configuration of the fibers affected the radar wave absorption properties. From Figure 5 we can see that the reflectivity of the nonwoven was lower than that of unwound fibers and nonwoven had good camouflage effect at high frequency. The reason was, on the one hand, that the fibers of nonwoven was woven tightly by needle, so the number of the fibers of needle-punched nonwoven was more than that of the unwound fibers in unit volume, which resulted in the electromagnetic loss increase. On the other hand, the3-D network needled-punched nonwoven was full of interspaces, which was favorable for the concussion and loss the radar wave. So all the fibers sample for the wave-absorbing test were made into needle-punched nonwoven (shown in Fig. 6) with 1.5 mm thick and 380 g/m^2 surface density by DILO needle-punched machine.

TABLE III
The Results of DSC

Sample	Melting point, T_m (°C)	T_{onset} (°C)	Heat of fusion (J/g)	Crystallinity of PP (%)
C0S0	164.02	153.0	109.40	52.15
C20S0	164.95	154.02	117.46	56.20
C40S0	162.05	152.62	115.23	55.13
C20S5	165.95	154.06	118.62	56.76
C20S10	167.60	160.21	120.70	57.75

Figures 7and 8 show variations of complex permeability ($\mu = \mu' + j\mu''$) of fiber with the Mn-Zn ferrite and Ba ferrite/Mn-Zn ferrite (Ba/Mn-Zn ferrite), respectively. Complex permittivity ($\varepsilon = \varepsilon' + j\varepsilon''$) of the fiber with the various content of bronze and 20 wt % Ba/Mn-Zn ferrite is shown in Figure 9. When the Ba/Mn-Zn ferrite was filled into the fiber, the complex permeability substantially increased compared with that of fiber with single Mn-Zn ferrite, as shown in Figures 7 and 8. This may be because the natural resonance absorption was increased by the increase of anisotropy that was increased by the addition of big anisotropy Ba ferrite powder. It can be seen from Figure 9 that complex permittivity of fiber with 5 and 15 wt % bronze was lower than that of the fiber with 20 wt % bronze. Furthermore, the research found that the MSER of fibers filled with 5, 15, and 20 wt % bronze was 1.68×10^8, 3.26×10^7, and 1.37×10^7 Ω g/cm^2, respectively. So, we concluded that

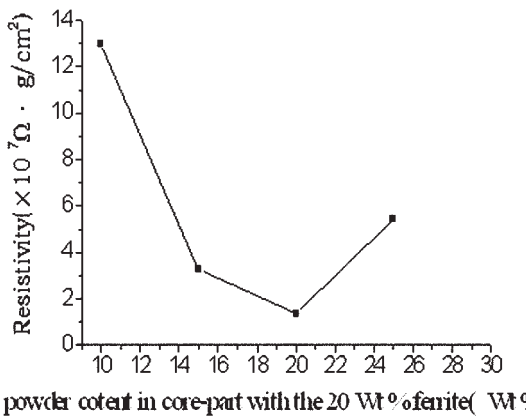

Figure 4 The relation of MSER of fibers and the bronze metal particles content.

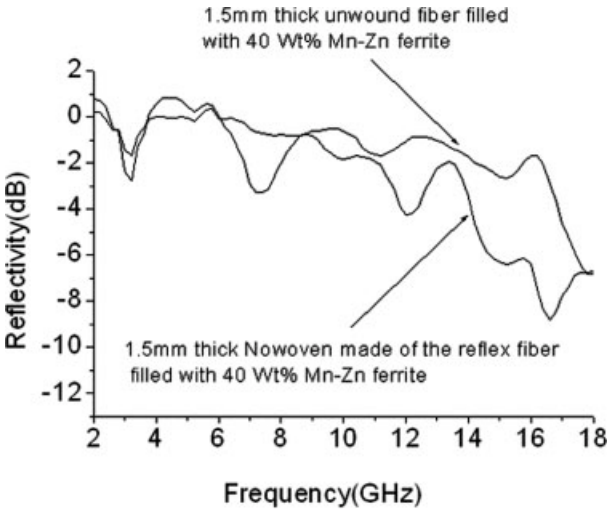

Figure 5 The effect of configuration on reflectivity.

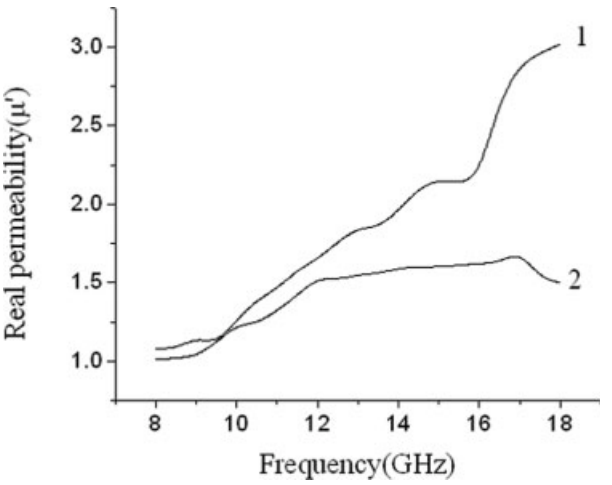

Figure 7 The real permeability of fiber with the (1) Ba/Mn-Zn ferrite; (2) Mn-Zn ferrite.

the complex permittivity was directly proportional to the conductance. The result was in accordance with the findings of Mouchon and Colomban.[18]

The Figures 10 and 11 give the outlines of the reflectivity of various fibers with ferrite and bronze. In Figure 10, the lowest reflectivity of fiber with 40 wt % Ba/Mn-Zn ferrite was 9.47 dB and 5 dB absorbing bandwidth was 5.95 GHz, while the lowest reflectivity of fiber containing 40 wt % Mn-Zn ferrite was only 4.22 dB. The reflectivity decrease may be explained by the increasing magnetic loss caused by the permeability rise, as shown in Figures 7 and 8. In the case of fibers filled with 20 wt % Ba/Mn-Zn ferrite and bronze absorption agents, the wave absorption properties of the fibers was improved with the bronze content increase (Fig. 11). The least reflectivity of the fibers filled with 5 and 15 wt % bronze was −2.92 dB and −7.82 dB, respectively, and 10 dB absorption bandwidth was 0, while the least reflectivity of the fibers filled with 20 wt % bronze reached −12.59 dB, and 10 dB absorption bandwidth was 2.39 GHz. The increase of bronze contents in fillers broadened the absorption bandwidth. This may be explained by the following three reasons. Firstly, the conductance was increased that resulted in the electric loss increasing with the addition of bronze particles. Secondly, the increscent dielectric loss contributed to the decrease in reflectivity, as shown in Figure 9. Moreover, the bronze particles cooperating with the ferrite should also explain the reasonable absorption. As we all know, the Rayleigh scattering will occur only when the incident electromagnetic wave with its wavelength more than the particles size impinges on the smaller particles. The bronze particles size was about 10^{-6} m, while the radar wavelength was from 15×10^{-2} m to 1.67×10^{-2} m (2–18 GHz). So the Rayleigh scattering was going to happen when the radar wave impinged on the small metal particles. The widespread and almost isotropic Rayleigh scattering waves were absorbed uniformly by the Ba/Mn-Zn ferrite in all directions. So the input of

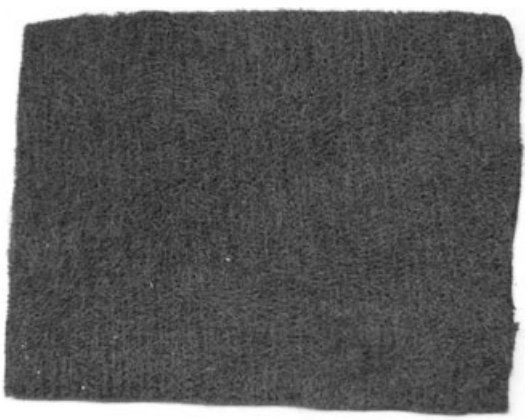

Figure 6 The photograph of nonwoven fabric sample.

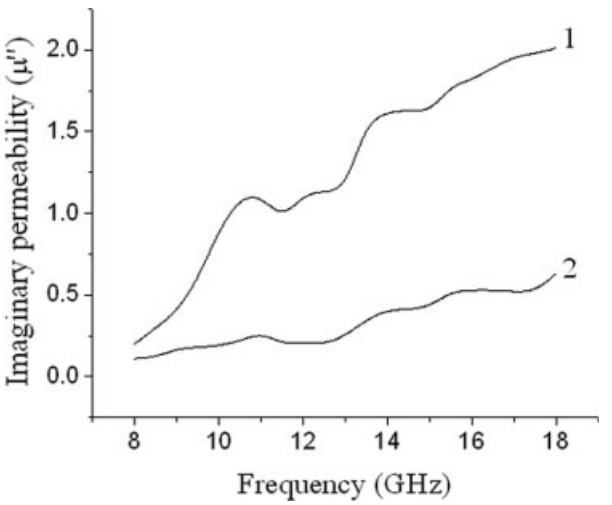

Figure 8 The imaginary permeability of fiber with the (1) Ba/Mn-Zn ferrite; (2) Mn-Zn ferrite.

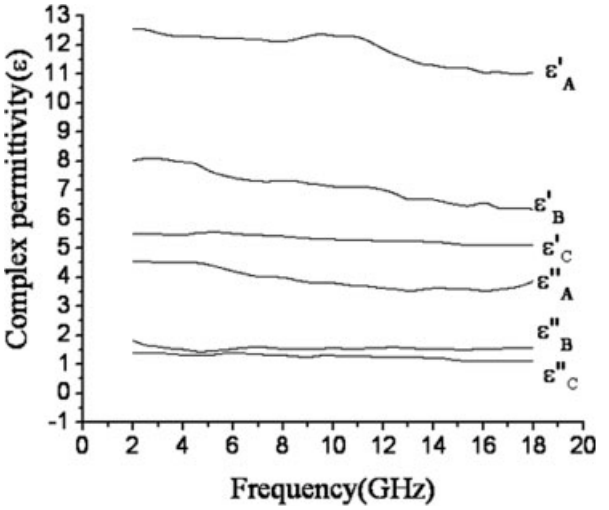

Figure 9 The complex permittivity of fiber containing 20 wt % Ba/Mn-Zn ferrite with (A) 20 wt % bronze; (B) 15 wt % bronze; (C) 5 wt % bronze.

bronze particles in the fibers made the absorption wave performance improved.

The compatibility of the fibers with infrared camouflage

As the radar absorbs bicomponent fibers with infrared camouflage, it should be compatible with the infrared camouflage. The Figure 12 shows the reflectivity of the fibers filled with the aluminum nanoparticles in the sheath-part and the fibers without the aluminum nanoparticles in the sheath-part. As shown in Figure 12, the reflectivity of the fibers changed very little with the aluminum nanoparticles input in the sheath-part. It means that the fibers have good compatibility with the infrared camouflage.

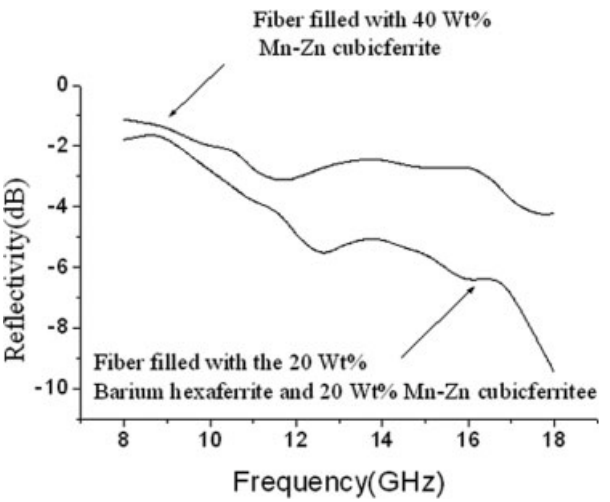

Figure 10 The reflectivity drawing of fiber with Ba/Mn-Zn ferrite and Mn-Zn ferrite.

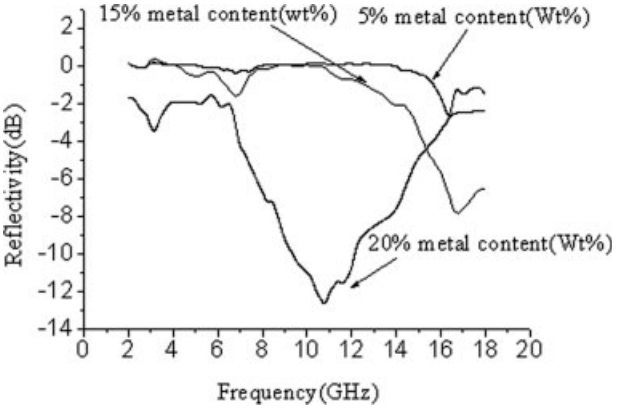

Figure 11 The effect of metal content in the core-part on reflectivity of the fibers containing 20 wt % Ba/Mn-Zn ferrite.

The infrared camouflage property

The Figure 13 indicates the infrared emissivity curves of the bicomponent fiber with Al particles in the sheath-part. The results showed that the input of the Al particles made the infrared emissivity of the fiber fall sharply and the infrared emissivity reached the lowest value of 0.62 when the Al content was 15 wt %. Then the infrared emissivity of the fiber tended toward invariability. We can interpret the results of experiments as follows. As we all know, the sum of the emissivity and reflectivity is 1 for the opacity materials. The reflectivity of Al is very high, which means it has very low emissivity. Besides, surface effect and microdimension effect of the nanoparticles also led to the decrease of infrared emissivity. So the Al can adjust the infrared emissivity of PP. But too many Al nanoparticles may agglomerate each other, which made the emissivity increase and also made against the radar-absorbing. So, as the research of Supcoe showed,[19,20]

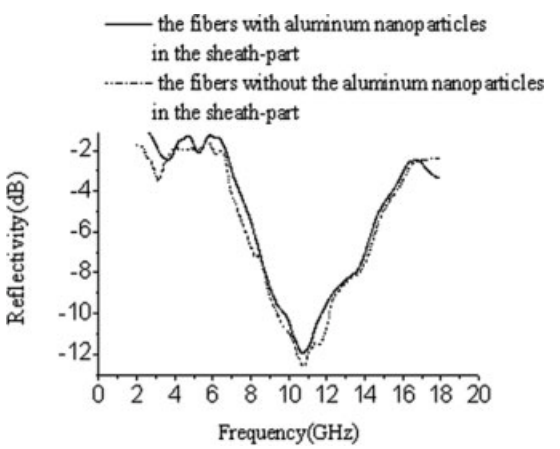

Figure 12 The reflectivity curves of bicomponent fibers filled with aluminum nanoparticles and bicomponent fibers without aluminum nanoparticles in the sheath-part.

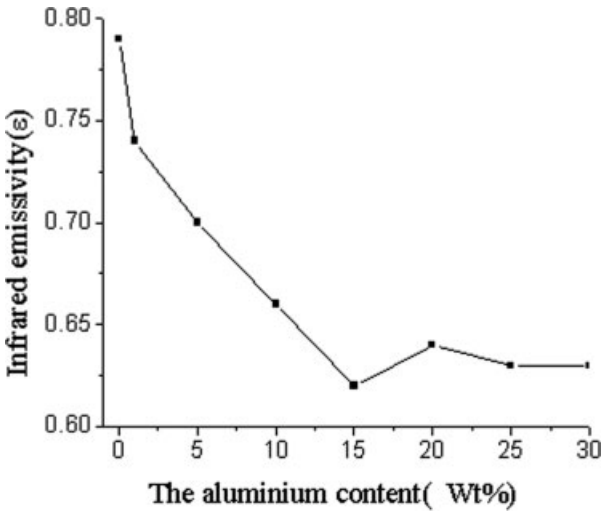

Figure 13 The changes of infrared emissivity of the fiber with the addition of Al particles.

the optimal content should be kept at 15–20 wt % in the sheath-part of fiber.

CONCLUSIONS

The sheath-core bicomponent fibers were melt-spun by coextrusion of polypropylene and polypropylene/various fillers master-batches. Crystallinity of bicomponent fibers with wave absorption agent and with nanoparticles was more than that of PP alone. The electrical resistance of fibers containing bronze particles in the core part reached minimum at the 20 wt % bronze content. The complex permeability of fiber with Mn-Zn ferrite increased by the addition of Ba ferrite and the complex permittivity of fiber containing the 20 wt % Ba/Mn-Zn ferrite was enhanced with the increasing bronze content. Fibers with Ba/Mn-Zn ferrite and bronze absorption agents showed good radar absorption effects. The aluminum nanoparticles in the sheath-part of the fibers had very limited effect on the wave-absorbing properties of the fibers. The infrared emissivity of the bicomponent fibers reached 0.62. As a result, it is possible to make a new light, thin, and high-performance radar/infrared multifunctional camouflage material with the new fiber.

References

1. Vinoy, K. J.; Jha, R. M. Radar Absorbing Materials from Theory to Design and Characterization; Kluwer: Boston, 1996.
2. Stonier, R. A. SAMPE J 1991, 27, 9.
3. Osamu, F.; Kei, K. Electr Eng Jpn 2002, 138, 34.
4. Im, J. I.; Kim, C. W.; Oh, T. S. J Korean Ceram 1999, 6, 571.
5. Yu, X. L.; Zhang, X. C. Mater Des 2002, 23, 51.
6. Sha, Y.; Jose, K. A.; Neo, C. P. Microwave Opt Technol Lett 2002, 32, 245.
7. Pomfret, S. J.; Adams, P. N.; Comfort, N. P.; Monkman, A. P. Synth Met 1999, 101, 724.
8. Zabetakis, D.; Dinderman, M.; Schoen, P. Adv Mater 2005, 17, 734.
9. Kim, S. H.; Seong, J. H.; Oh, K. W. J Appl Polym Sci 2002, 83, 2245.
10. Dhawan, S. K.; Singh, N.; Venkatachalam, S. Synth Met 2002, 129, 261.
11. Jim, G. Eng Technol 2004, 7, 16.
12. Rao, G. A.; Mahulikar, S. P. Aeronaut J 2002, 106, 629.
13. Brandrup, J.; Immergut, E. H.; Grulke, E. A. Polymer Handbook; Wiley: New York, 1999.
14. Sang, Y. Y.; Sung, H. J. Polym Int 2003, 52, 1053.
15. Yang, F.; Ou, Y.; Yu, Z. J Appl Polym Sci 1998, 69, 355.
16. Monserrat, G. Polym Adv Technol 2004, 15, 164.
17. Faez, R.; Gazotti, W. A.; De Paoli, M. A. Polymer 1999, 40, 5497.
18. Mouchon, E.; Colomban, P. J Mater Sci 1996, 31, 323.
19. Supcoe, R. F. U.S. Pat. 4,289,677 (1981).
20. Supcoe, R. F. U.S. Pat. 4,311,623 (1982).